Revue des Energies Renouvelables Vol. 15 N°2 (2012) 305 - 320

Sliding mode control of brushless doubly-fed machine used in wind energy conversion system

H. Serhoud* and D. Benattous†

Institute of Science Technology, University Center of El-Oued, Algeria

(reçu le 30 Mars 2009 - accepté le 30 Mars 2012)

Résumé - *Cet article présente les applications de la commande par mode glissement sur une génératrice asynchrone sans balais doublement alimentée (BDIG) utilisée dans les systèmes de conversion d'énergie éolienne. Le contrôleur est conçu sur la base du contrôle en mode glissement combiné avec la technique du principe d'orientation du flux du bobinage de puissance Le contrôle indépendant des puissances active et réactive a été développé et les performances des systèmes de conversion d'énergie éolienne proposées est validé dans l'environnement Matlab/Simulink. Les résultats de simulation numérique obtenus confirment l'efficacité de cette stratégie de contrôle.*

Abstract - *This paper presents the applications of the sliding mode control to a brushless doubly fed induction generator (BDFG) used in wind-energy conversion systems. The controller is designed based on the sliding mode control combined with a the stator power winding flux oriented vector principle, the independent control of active and reactive powers has been developed and the performance of proposed the block diagram of the variable speed constant-frequency (VSCF) wind energy generation system is validated in the Matlab/Simulink environment and the computer simulation results obtained confirm the effectiveness of this control strategy.*

Keywords: Brushless doubly fed Machine (BDFM) - Sliding mode control - Maximum wind power generation - Back-to-back PWM converter.

1. INTRODUCTION

Recent research has illustrated the advantages of the brushless doubly-fed machine (BDFM) in motor drive and generator system applications promise significant advantages for wind power generation, as they offer high reliability and low maintenance requirements by virtue of absence of a brush gear [6].

The BDFM which is also known as a self-cascaded machine is composed of two three-phase windings in the stator of different pole numbers (called power winding PW and control winding CW) and a special rotor winding. Typically the two stator supplies are of different frequencies, one a fixed frequency supply connected to the grid, and the other a variable frequency supply derived from a power electronic frequency converter (inverter), as illustrated in figure 1. The natural synchronous speed of the machine equal to:

$$\omega_r = \frac{\omega_p \pm \omega_c}{p_p + p_c} \tag{1}$$

* hichamser_39@yahoo.fr
† dbenattous@yahoo.com

Where ω_p and ω_c are the electrical angular velocities of the PW and CW voltages. The control winding is connected to grid by two voltage-source PWM converter with back-to-back connection. The converter contains the rectifier and inverter, with an intermediate DC voltage link. The DC-link created by the capacitor in the middle decouples the operation of the two converters.

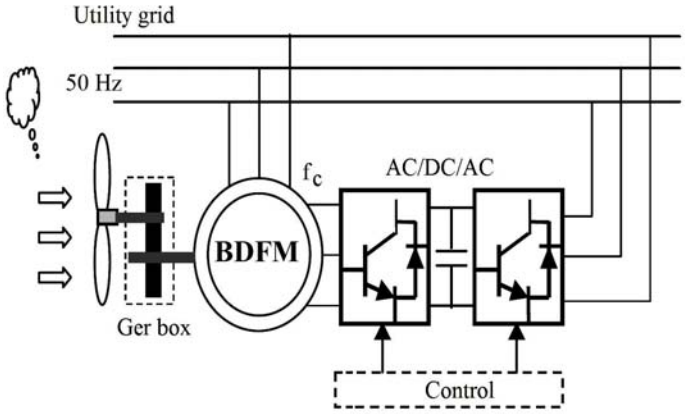

Fig. 1: Configuration of a BDFG wind energy conversion system using back-to-back converter

This configuration finds an interesting in energy generations applications especially in variable speed system, when the converter has to operate with reverse power direction which leads to back-to-back converter is that it allows for true four-quadrant operation, meaning that the direction of the active power flow can be reversed at any instant.

The variable speed constant frequency (VSCF) is the most interesting if the nature of wind with the capability of wind generating systems constantly increasing. It is more important to improve the efficiency by capture the maximum wind energy and use the high quality, efficient and controllable where the major challenge is independent control of active and reactive powers exchanged between the BDFG and the grid.

The different control strategies that have been used until now in the BDFM are the scalar current control [8], the direct torque control [20], L2 robust control method [18], H∞ control[19], fuzzy power control [9, 18], sliding mode power control [19], the rotor flux oriented controlled [3], a new vector controller using a dynamic model with a unified reference frame based on the power winding flux was investigated for the BDFM by Poza [13], and a simplified controller oriented with the power winding stator flux with a complete mathematical derivation frame presented by Shiyi [6, 7] with some experimental results presented on both speed and reactive power regulating.

A sliding mode control of active and reactive power for BDFM using a dynamic model with the rotor reference frame is proposed in [3]. In this paper a new variable structure controller using a dynamic model with a unified reference frame based on the power winding flux oriented controlled is proposed, the SMC control is conception for the power loop of the outer loop associated to power flux oriented vector control scheme.

Based on the control principles defined in Shiyi [16], and to make it easy for the system to implement maximal power point tracking (MPPT), when the power winding is directly connected to the grid while the control winding is connected to the grid through back-to-back converters when the power flows between BDFG and utility grid are discussed. The extensive simulation study in the beginning validated all the control algorithms.

2. CONTROL MECHANISM OF THE MAXIMAL WIND ENERGY CAPTURING

Wind energy is captured by the blades of the wind turbine and is turned into mechanical torque on the hub. From Betz theory, the capture power got from wind energy by wind turbine can be expressed as [17, 18]

$$P = \frac{\pi}{2} \times C_p \times R^2 \times \rho \times v^3 \tag{2}$$

Where ρ is the air density, R is the turbine radius and v the wind velocity, further the power coefficient Cp is a function of the tip speed ratio ($\lambda = \omega_t R / v$) as well as the blade pitch angle β, ω_t is the angular speed of the wind turbine.

$$C_p(\lambda,\beta) = 0.5176 \times \left(\frac{116}{\lambda_i} - 0.4\beta - 5 \right) \times e^{-\frac{21}{\lambda_i}} + 0.0068\lambda \tag{3}$$

Where, $$\frac{1}{\lambda_i} = \frac{1}{\lambda + 0.08\beta} - \frac{0.035}{\beta^3 + 1} \tag{4}$$

Figure 2 shows the Power-Speed characteristics of the wind turbine, the peak power for each wind speed occurs at the point where C_p is maximized. To maximize the power generated, it is therefore desirable for the generator to have a power characteristic that will follow the maximum C_{p-max} line.

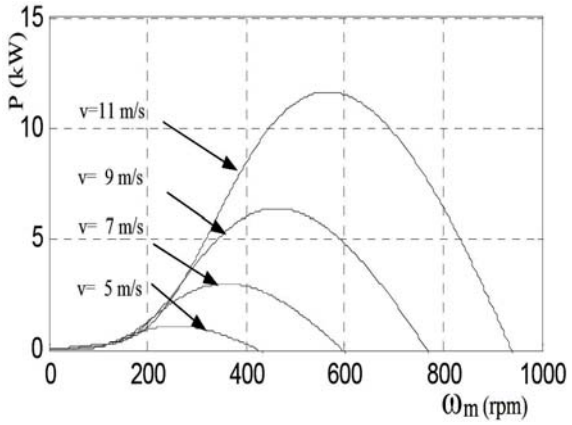

Fig. 2: Wind turbine generator power- rotor speed characteristics

To extract the maximum power generated, we must maintain λ at the optimal command rotor speed λ_{opt}. The coordinates of the optimal point is the maximum power coefficient C_p are (λ_{opt} = 8.1, C_{p-max} = 0.48, β = 0). Increasing β allows the reduction of mechanical power recovered from the axis of the wind turbine.

In this paper the maximizing power with control of the speed is used, it is assumed that the electromagnetic torque developed by the machine is equal to its reference value whatever the power generated.

The estimate of the reference speed of the turbine can be obtained by:

$$\omega_t = \frac{\lambda_{opt} \times v}{R} \tag{5}$$

Where the relation of the wind turbine speed and the generator speed is as follows:

$$\omega_m = G \times \omega_t \tag{6}$$

The action of the speed corrector must achieve control the mechanical speed ω_m with its reference ω^*_m.

The electromagnetic torque reference is defined as

$$T^* = \left(k_p + k_i \int \right) \times \left(\omega^*_m - \omega_m\right) \tag{7}$$

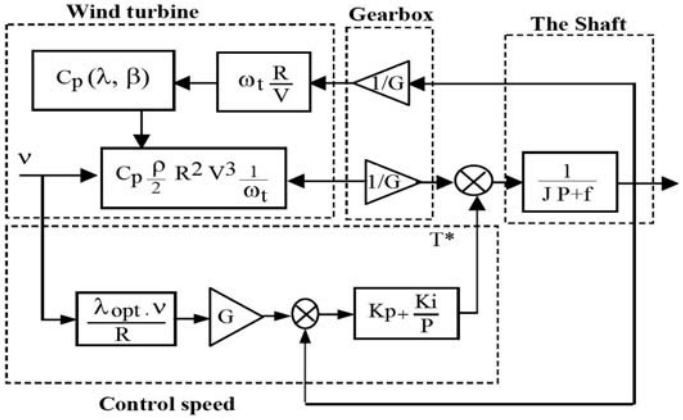

Fig. 3: Device control with control speed

3. MATHEMATICAL MODEL

The model of the BFIM in the power winding flux frame is expressed as [4], [7], [12]:

$$V_p = R_p \times i_p + \frac{d\Psi_p}{dt} + j \times \omega_p \times \Psi_p \tag{8}$$

$$V_c = R_c \times i_c + \frac{d\Psi_c}{dt} + j \times (\omega_p - (P_p + P_c) \times \omega_r) \times \Psi_c \tag{9}$$

$$V_r = R_r \times i_r + \frac{d\Psi_r}{dt} + j\times(\omega_p - P_p \times \omega_r)\times\Psi_r \quad (10)$$

The flux equations are given as:

$$\Psi_p = L_p \times i_p + M_p \times i_r \quad (11)$$

$$\Psi_c = L_c \times i_c + M_c \times i_r \quad (12)$$

$$\Psi_r = L_r \times i_r + M_c \times i_c + M_p \times i_p \quad (13)$$

The electromagnetic torque is expressed as [18]:

$$T_e = \frac{3}{2}\times p_p \times M_p \times (i_{qp} \times i_{dr} - i_{dp} \times i_{qr}) - \frac{3}{2}\times p_c \times M_c \times (i_{qc} \times i_{dr} - i_{dc} \times i_{qr}) \quad (14)$$

The active and reactive powers of power winding are defined as:

$$P_p = \frac{3}{2}\times(V_{dp} \times i_{dp} + V_{dp} \times i_{qp}) \quad (15)$$

$$Q_p = \frac{3}{2}\times(V_{qp} \times i_{dp} + V_{dp} \times i_{dp}) \quad (16)$$

4. SLIDING MODE POWER CONTROLLER DESIGN

Recently sliding mode power controllers have been introduced in the control of doubly fed induction generator [1, 2]. Brushless doubly Fed Induction generator in [19] they have the advantage to be robust and its strongest justification to the problem of use of a robust non-linear control law for the model uncertainties.

In this paper the sliding mode conception using the model of BDFG in (d-q) reference with the power winding flux vector aligned with d-axis.

4.1 Control of the BDFM with a power winding field oriented

If the d-axis of the power winding synchronous reference frame is aligned with the power winding air gap flux the power winding R_p is neglected, then there is relation between the power winding voltage and its flux:

$$\begin{cases} V_{dp} = 0 \\ V_{qp} = V_p = \omega_p \times \Psi_p \end{cases} \quad (17)$$

$$\begin{cases} \Psi_p = L_p \times i_{dp} + M_p \times i_{dr} \\ 0 = L_p \times i_{qp} + M_p \times i_{qr} \end{cases} \quad (18)$$

From (18), the equations linking the rotor currents to the power winding currents are deduced as below:

$$\begin{cases} i_{dr} = \dfrac{\Psi_p}{M_p} - \dfrac{L_{dp}}{M_p} \times i_{dp} \\ i_{qr} = -\dfrac{L_{qp}}{M_p} \times i_{qp} \end{cases} \tag{19}$$

4.2 PW flux estimator

Form of PW voltage equation shown (8) its derivation in the stationary reference frame ($\alpha - \beta$ reference frame) is given as follows:

$$\begin{cases} \Psi_{\alpha p} = \int (V_{\alpha p} - R_p \times i_{\alpha p}) \times dt \\ \Psi_{\beta p} = \int (V_{\beta p} - R_p \times i_{\beta p}) \times dt \end{cases} \tag{20}$$

The PW flux angle can be expressed as:

$$\theta_p = \arctan \frac{\Psi_{\beta p}}{\Psi_{\alpha p}} \tag{21}$$

4.3 Control of power winding current

Suppose that the BDFM is running in steady state, then the dynamic model can be transferred to the state model [7], [19].

$$\begin{cases} V_{dp} = R_p \times i_{dp} - \omega_p \times L_p \times i_{qp} - \omega_p \times M_p \times i_{qr} \\ V_{qp} = R_p \times i_{qp} + \omega_p \times L_p \times i_{dp} + \omega_p \times M_p \times i_{dr} \end{cases} \tag{22}$$

$$\begin{cases} \dfrac{S_2}{S_1} \times V_{dc} = \dfrac{S_2}{S_1} \times R_c \times i_{dc} - \omega_p \times L_c \times i_{qc} - \omega_p \times M_c \times i_{qr} \\ \dfrac{S_2}{S_1} \times V_{qc} = \dfrac{S_2}{S_1} \times R_c \times i_{qc} + \omega_p \times L_c \times i_{dc} + \omega_p \times M_c \times i_{dr} \end{cases} \tag{23}$$

$$\begin{cases} 0 = \dfrac{1}{S_1} \times R_r \times i_{dr} - \omega_p \times L_r \times i_{qr} - \omega_p \times M_c \times i_{qc} - \omega_p \times M_p \times i_{qp} \\ 0 = \dfrac{1}{S_1} \times R_r \times i_{qr} + \omega_p \times L_r \times i_{dr} + \omega_p \times M_c \times i_{dc} + \omega_p \times M_p \times i_{dp} \end{cases} \tag{24}$$

S_1 , S_2 are the slips, which are defined as:

$$S_1 = \frac{\omega_p - p_p \times \omega_p}{\omega_p}, \; S_2 = \frac{\omega_c - p_p \times \omega_p}{\omega_c} \tag{25}$$

Equation (26), (27) can be obtained by combining equation (22) with equation (24) and considering equation (18), (20) and neglecting the power winding resistance

$$i_{dc} = \left(\frac{L_r L_p - M_p}{M_p \times M_c} \right) \times i_{dp} - \frac{\Psi_p L_r}{M_p \times \omega_p \times M_c} + \frac{R_r L_p}{M_p \times M_c \times \omega_p \times S_1} \times i_{qp} \tag{26}$$

$$i_{qc} = \left(\frac{L_r L_p - M_p}{M_p \times M_c} \right) \times i_{qp} + \frac{\Psi_p R_r}{M_p \times \omega_p \times S_1 \times M_c} - \frac{R_r L_p}{M_p \times M_c \times \omega_p \times S_1} \times i_{dp} \quad (27)$$

Equation (15), (26) represents the relationship of the power current and control wind current.

The first term of equation (25), (26) defines the direct coupling between i_c, i_p. The second term, performs as a constant and the third term reflects the cross coupling.

4.4 Control of power control current

Combining with equations (9), (12), (19), (24), the control winding voltage can be derived as:

$$\begin{aligned} V_{dc} = R_c \times i_{dc} + \left(L_c - \frac{M_c^2}{L_r} \right) \times \frac{di_{dc}}{dt} - \frac{M_c \times R_r \times L_p}{\omega_p \times L_r \times S_1 \times M_p} \times \frac{di_{qp}}{dt} \\ - \frac{M_c \times M_p}{L_r} \times \frac{di_{dp}}{dt} + (\omega_p - (p_p + p_c) \times \omega_r) \times \left(L_c \times i_{qc} + M_c \times \left(- \frac{L_{qp}}{M_p} \times i_{qp} \right) \right) \end{aligned} \quad (28)$$

$$\begin{aligned} V_{qc} = R_c \times i_{qc} + \left(L_c - \frac{M_c^2}{L_r} \right) \times \frac{di_{qc}}{dt} - \frac{M_c \times R_r \times L_p}{\omega_p \times L_r \times S_1 \times M_p} \times \frac{di_{qp}}{dt} \\ - \frac{M_c \times M_p}{L_r} \times \frac{di_{qp}}{dt} + (\omega_p - (p_p + p_c) \times \omega_r) \times \left(L_c \times i_{qc} + M_c \times \left(\frac{\Psi_p}{M_p} - \frac{L_{dp}}{M_p} \times i_{dp} \right) \right) \end{aligned} \quad (29)$$

The first term, $R_c \times i_{qc} + \left(L_c - \frac{M_c^2}{L_r} \right) \times \frac{di_{qc}}{dt}$ shows the relation between V_{qc} with i_{qc}

The second term, $- \frac{M_c \times R_r \times L_p}{\omega_p \times L_r \times S_1 \times M_p} \times \frac{di_{qp}}{dt} - \frac{M_c \times M_p}{L_r} \times \frac{di_{qp}}{dt}$ represents the cross coupling it can be neglected in steady state.

The third term, $- (\omega_p - (p_p + p_c) \times \omega_r) \times \left(L_c \times i_{qc} + M_c \times \left(\frac{\Psi_p}{M_p} - \frac{L_{dp}}{M_p} \times i_{dp} \right) \right)$ shows another cross coupling, it can be neglected compared with the direct coupling term.

4.5 Sliding mode power control

The basic principle of the sliding mode control consists in moving the state trajectory of the system toward a surface $S(X) = 0$ and maintaining it around this surface with the switching logic function U_n, where U_n is a sign function defined as:

$$U_n = \operatorname{sgn}(S(X)) = \begin{cases} 1 & \text{if} \quad S(X) < 0 \\ -1 & \text{if} \quad S(X) > 0 \end{cases} \quad (30)$$

In this paper the corresponding references are calculated according to the references of active and reactive power using the model of BDFG in (d-q) reference with the power winding flux vector aligned with d-axis.

Tacking into consideration the chosen reference frame, the active and reactive powers at the power winding can be written as follows:

$$\begin{cases} P_p = \frac{3}{2} \times V_{qp} \times i_{qp} \\ Q_p = \frac{3}{2} \times V_{qp} \times i_{dp} \end{cases} \quad (31)$$

The paper designs the following sliding mode, let:

$$\begin{cases} S_1 = P^* - P_p \\ S_2 = Q^* - Q_p \end{cases} \quad (32)$$

Where P^* and Q^* are the expected active power and reactive power reference.

It takes the current expression of i_{dc}, i_{qc}, with the power equation (31) and tacking into consideration the sliding mode in the steady state ($S = 0$, $\dot{S} = 0$).

The equivalent control winding current vector U^{eq} can express by:

$$U_{dc}^{eq} = \frac{2}{3} \times \left(\frac{L_r L_p - M_p}{M_p \times M_c} \right) \times \frac{P_p}{V_{qp}} - \frac{\Psi_p \times L_r}{M_p \times \omega_p \times M_c} + \frac{2}{3} \times \frac{R_r \times L_p}{M_p \times \omega_p \times M_c \times S_1} \times \frac{P_p}{V_{qp}} \quad (33)$$

$$U_{qc}^{eq} = \frac{2}{3} \times \left(\frac{L_r L_p - M_p}{M_p \times M_c} \right) \times \frac{P_p}{V_{qp}} + \frac{\Psi_p \times R_r}{M_p \times \omega_p \times M_c \times S_1} + \frac{2}{3} \times \frac{R_r \times L_p}{M_p \times \omega_p \times M_c \times S_1} \times \frac{Q_p}{V_{qp}} \quad (34)$$

The control vector is shown below:

$$U = U^{eq} + U^n \quad (35)$$

U^n is the Sign function defined by:

$$U^n = -K \times \text{sign}(S) \quad (36)$$

Where K determine the ability of overcoming the chattering.

In order to reduce the chattering phenomenon due to the discontinuous nature of the controller, a smooth function is defined in some neighbourhood of the sliding surface with a threshold as seen in figure 4.

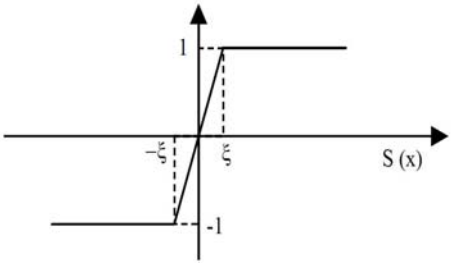

Fig. 4: Sketch of the saturation function

An integral action is now added to the control in order to reduce the gain of the "sign" function and then reduce the chattering effect. This action will also improve the controllers performances in terms of reference tracking [2].

The integral surface form is given by:

$$\eta = K_{\eta} \times \int_{0}^{t} S \times dt \tag{37}$$

The integral function is added during the positive phase of the sliding surface, the equivalent control will have the following form:

$$U = U^{eq} + U^{n} + \eta \tag{38}$$

The SMC control is conception for the power loop of the outer loop associated to power flux oriented vector control scheme, to further enhance the robustness of the system path as shown in Figure 5.

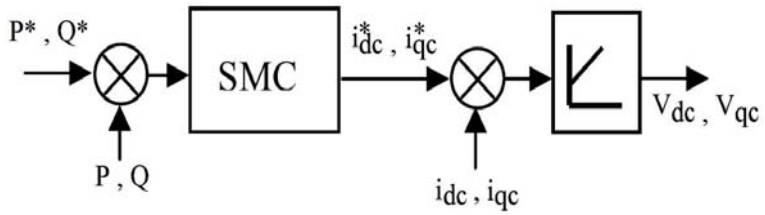

Fig. 5: Control scheme

5. CONTROL OF THE GRID INVERTER

The aids of grid-side converter control system are providing bi-directed power flowed channel for control winding - grid-side converter, the grid side three-level converter is to regulate the dc-link voltage and to set a unit power factor [17].

The model of the system is given by the following equation:

$$\frac{d}{dt}\begin{bmatrix} i_a \\ i_b \\ i_c \end{bmatrix} = -\frac{R}{L}\begin{bmatrix} 1 & 0 & 0 \\ 0 & 1 & 0 \\ 0 & 0 & 1 \end{bmatrix}\begin{bmatrix} i_a \\ i_b \\ i_c \end{bmatrix} + \frac{1}{L}\begin{bmatrix} V_{a-} & V_{an} \\ V_{b-} & V_{bn} \\ V_{c-} & V_{cn} \end{bmatrix} \tag{39}$$

The dc capacitor voltage equation expressed using switching function is as follows

$$C \times \frac{dV_c}{dt} = i_a \times S_a + i_a \times S_a + i_a \times S_a - i_d \tag{40}$$

The voltage equations in the d-q synchronous reference frame are presented below:

$$\begin{cases} V_d = R \times i_d + L_p \times \dfrac{di_d}{dt} - \omega_s \times L \times i_{dr} + V_{dn} \\ V_q = R \times i_q + L_p \times \dfrac{di_q}{dt} - \omega_s \times L \times i_{dr} + V_{qn} \end{cases} \tag{41}$$

The direct axis current is used to regulate the reactive power and the quadratic axis current is used to regulate the DC-link voltage. The reference frame is considered oriented along the stator voltage vector. This method gives possibility to realise independent control of the active and reactive power between the GSC and the supply side.

For eliminating the current couple between d-axis and q-axis and disturbance of grid voltage, current feed-back values $\omega L i_q$ and $\omega L i_d$ are introduced as compensation components.

The control strategy of the total system can be implemented by voltage oriented control with PLL in the synchronous frame as presented in Fig. 6.

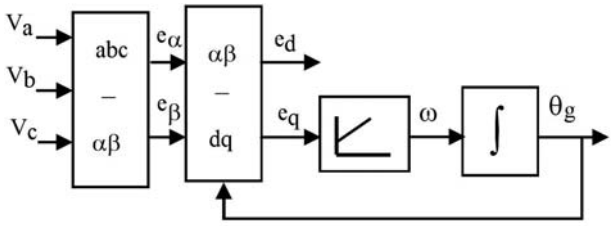

Fig. 6: The configuration of three phase PLL

Based on the above relations, the GSC control diagram can be easily deduced as presented in Fig. 7.

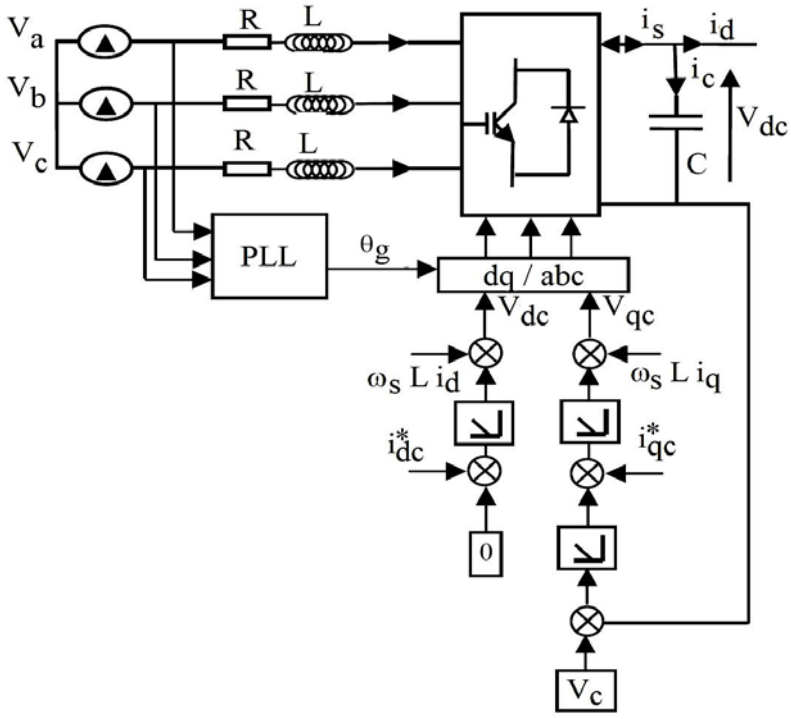

Fig. 7: Control diagram of the grid side converter

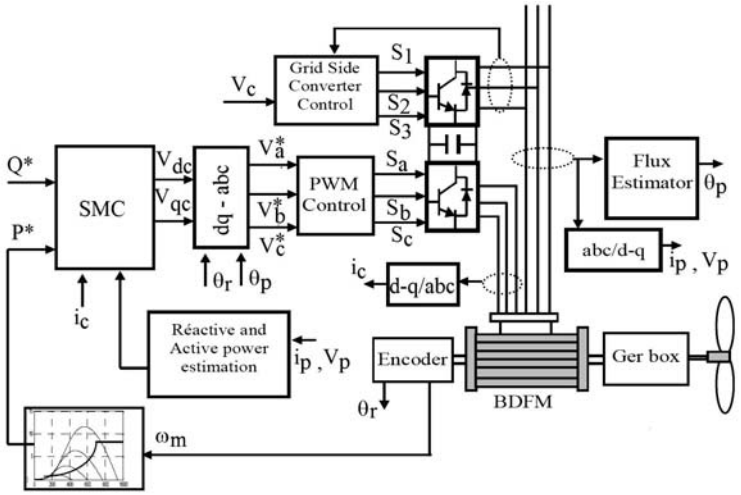

Fig. 8: Sliding mode control block diagram of BDFM

6. SIMULATION RESULTS

The analysis is evaluated through simulations in MATLAB®/Simulink® has been done with a ode 3, fixed-step solver with a step size of 2e-5s. The sample machine used in this simulation model is 3Y-3Y connected and its stator winding is 6-2 pole, the main parameters of BDFM simulation model are reported in **Table 1**.

The wind parameters are: $\beta = 0$, $R = 3$ m, the optimal tip speed ratio $\lambda = 8.1$, and the corresponding maximum power coefficient $C_{p-max} = 0.48$, otherwise the speed increase ratio of the gearbox $G = 2$.

The results of simulations are obtained with reactive power ($Q_p = 0$) (Fig. 12), and to evaluate the dynamic performance of maximum power point tracking of the system a step change in wind speed as shown in Figure 9.

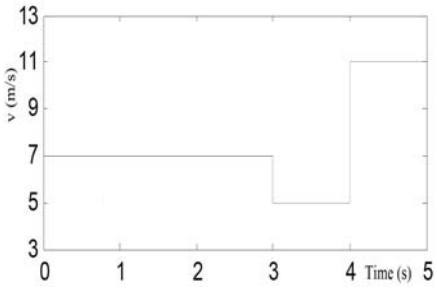

Fig. 9: Wind speed

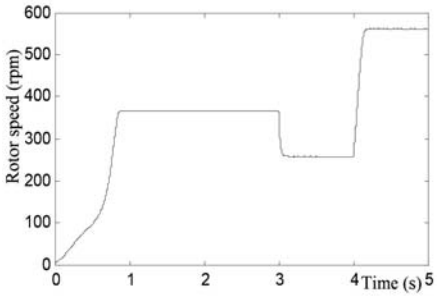

Fig. 10: Rotor speed

Fig. 10 is the optimal speed of rotor and it varies with the variable wind velocity.

The active and reactive stator powers and its references are reported in Fig 11, 12, these figures represent a good pursuit its references.

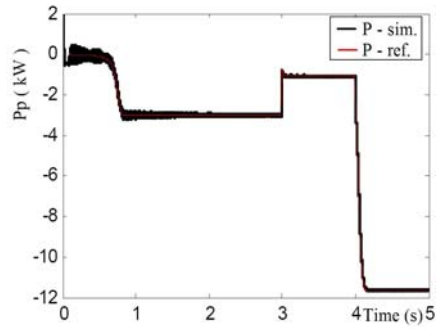

Fig. 11: The active power of PW

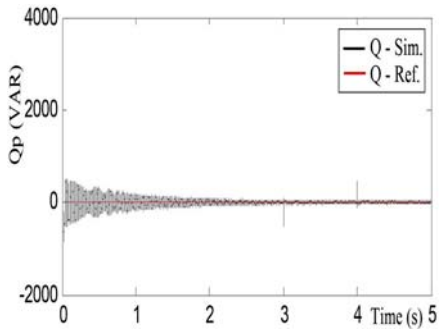

Fig. 12: The reactive power of PW

Fig. 13 shown the frequency and amplitude of the control winding current both change during the period of the active and reactive power variation. The Fig.14 shown the frequency of power winding current is constants accorder to power frequency of the grid with amplitude change when the reference of the active power is modified.

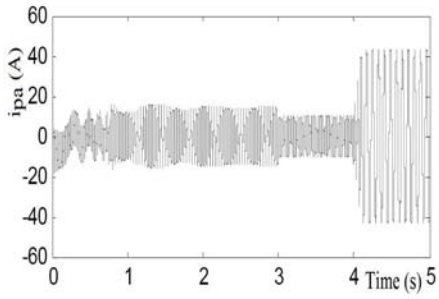

Fig. 13: Phase control winding

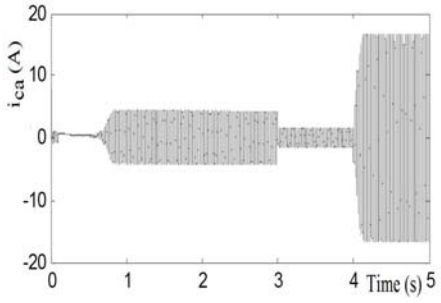

Fig. 14: Phase power winding current

Fig. 15 is validating the three phase PWM rectifier is simulated when the response of the DC voltage controller which provides a good tracking of its reference (600 V).

When the active power is increasing the DC voltage is trying also to increase. The DC controller is reducing very fast the error and is keeping always the DC link at the same reference value.

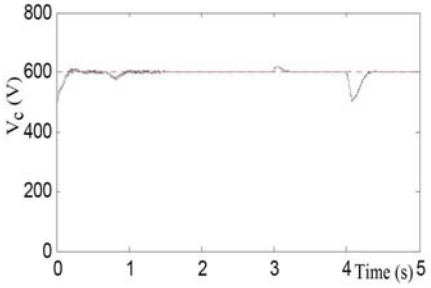

Fig. 15: DC voltage

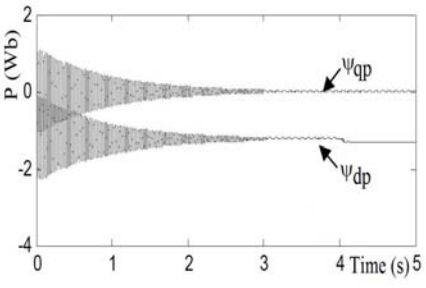

Fig. 16: Power winding flux

From the Fig 16, we can see that the power winding flux follows its reference axis (d) with a quadratic component near zero.

Fig 17 is the zoom of a stator power winding voltage and the corresponding current on the same time axis, it can be note that the fact unity power factor is guaranteed by the proposed controller.

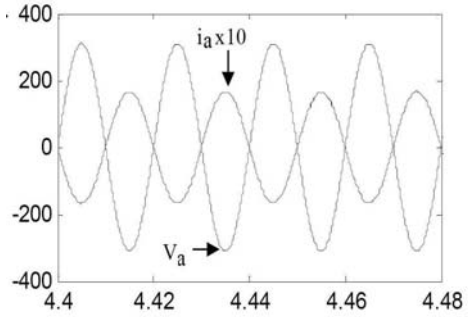

Fig. 17: Zoom of phase power winding current and voltage

In Fig. 18 it can be seen the grid currents which are increasing in function of the variation and respectively stator active power winding variation.

Fig. 19 shows when the first phase of the grid voltage is plotted together with the first phase of the grid current. It can be notice that the line current is nearly a sine wave with unity power factor.

Fig. 20 illustrates in detail the dynamic variation of the MPPT in wind speed change (7, 5, 11 m/s) in the rotor speed- power characteristics of BDFG-turbine.

It can be noted it is accorder with the optimal value, these results realize the maximum wind energy tracking control.

Fig. 21, Fig. 22 shows that, when the wind profile change, C_p can fast reach around the optimal value. The power coefficient is kept around its optimum $C_{p_{max}} = 0.48$ occurs at a $\lambda_{opt} = 8.1$.

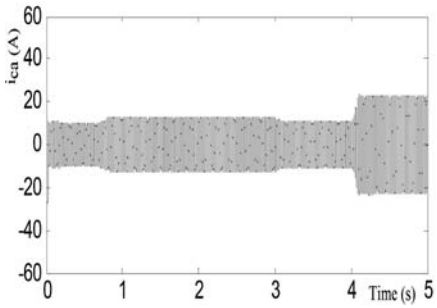

Fig. 18: Phase grid current

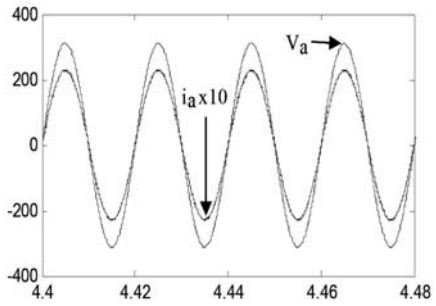

Fig. 19: Zoom of phase grid current and voltage

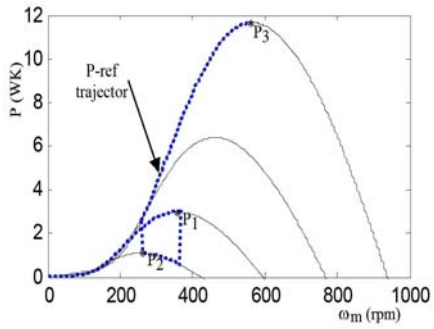

Fig. 20: Wind turbine maximum power trajectory

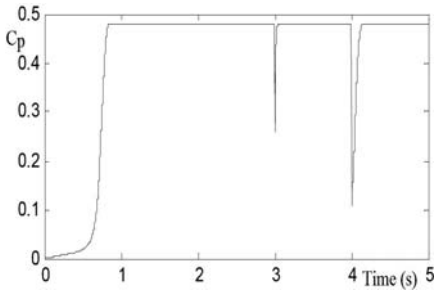

Fig. 21: Power coefficient C_p variation

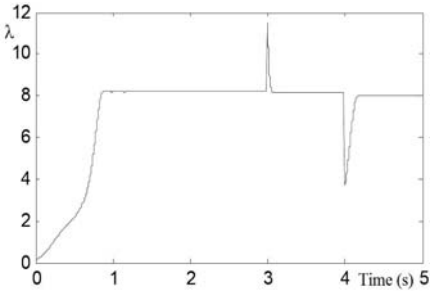

Fig. 22: The tip speed ratio λ

7. CONCLUSION

The aim of the paper develop the control decoupled the active and reactive of a grid connected BDFG by use the sliding mode control in the dynamic model with a unified reference frame based on the power winding flux oriented, when the control winding is connected to the grid via back-to-back converters. From simulation results, it can be concluded.

The conception of sliding mode control strategy associated to the vector controls techniques shown the good performance and the more reliability of the control when the system is tested under different wind speed when the maximal wind energy tracing is found.

Table 1: The electrical parameters of BDFM

	PW	CW	Rotor
Resistance (Ω)	R_p = 0.435	R_c =0.435	R_r =1.63
Self-Inductance (mH)	L_p =71.38	L_c =65.33	L_r =142.8
Mutual-Inductance (mH)	M_p =69.311	M_c =60.21	

BACK-TO-BACK PWM CONVERTER

Input AC rated phase-voltage: $V_{inp} = 220\,V / f = 50\,Hz$; DC link capacitance: $C = 0.002\,F, AC$; Filter inductance: $I = 0.014\,H$; Resistance: $r = 0.3\,\Omega$.

REFERENCES

[1] Jiabing Hu, Henng Nian, Bin Hu, Yikang He and Z.Q. Zhu, '*Direct Active and Reactive Power Regulation of DFIG Using Sliding-Mode Control Approach*', IEEE Transactions on Energy Conversion, Vol. 25, N°4, pp. 1028 - 1039, 2010.

[2] M. Machmoum and F. Poitiers, '*Sliding Mode Control of a Variable Speed Wind Ener.gy Conversion System with DFIG*', International Conference and Exhibition on Ecological Vehicles and Renewable Energies, EVER, March 26-29, 2009.

[3] D. Zhou, R. Spee, G.C. Alexander and A.K. Wallace, '*A Simplified Method for Dynamic Control of Brushless Doubly-Fed Machines*', Proceedings of the International Conference on Industrial Electronics, Control, and Instrumentation, Vol. 2, pp 946 - 951, Aug. 1996.

[4] J. Poza, E. Oyarbide, I. Sarasola and M. Rodriguez, '*Vector Control Design and Experimental Evaluation for the Brushless Doubly Fed Machine*', IET Electric Power Applications, Vol. 3, N°4, pp. 247 – 256, July 2009.

[5] Y. Liu, L. Yi and X. Zhao, '*Control of Brushless Doubly-fed Machine for Wind Power Generation Based on Two-stage Matrix Converter*', IEEE Asia-Pacific, Power and Energy Engineering Conference, APPEEC , pp. 1 - 5, 2009 .

[6] S. Shao, E. Abdi and R. McMahon, '*Vector Control of the Brushless Doubly-Fed Machine for Wind Power Generation*', IEEE International Conference on Sustainable Energy Technologies, ICSET 08, pp. 322 - 327, 2008.

[7] S. Shao, E. Abdi and R. McMahon, '*Stator-Flux-Oriented Vector for Brushless Doubly Fed Induction Generator*', IEEE Transactions On Industry Electronic ,Vol. 56, N°10, pp. 4220 – 4228, October 2009.

[8] Z. Sarasola, J. Poza, E. Oyarbide and M.A. Rodriguez, '*Stability Analysis of a Brushless Doubly-Fed Machine under Closed Loop Scalar Current Control*', Proceedings of the 32nd Annual Conference on IEEE Industrial Electronics, IECON-06, pp. 1527 - 1532, 2006.

[9] H. Shoudao, W. Yan, L. Youjie and W. Yaonan, '*Fuzzy-Based Power Factor Control for Brushless Doubly-Fed Machines*', Proceedings of the 4th World Congress on Intelligent Control and Automation, Shanghai. P.R. China, Vol. 1, pp. 587 – 591, 2002.

[10] Y. Liu, L. Yi and X. Zhao, '*Control of Brushless Doubly-fed Machine for Wind Power Generation Based on Two-stage Matrix converter*', Proceedings of Power and Energy Engineering Conference, APPEEC 2009, Asia-Pacific, pp. 1 – 5, March 27-31, 2009.

[11] L. Xu, L. Zhen and E-H. Kim, '*Field-Orientation Control of a Doubly Excited Brushless Reluctance Machine*', IEEE Transactions on Industry Applications, Vol. 34, N°1, pp. 148 – 155, 1998.

[12] J. Poza, E. Oyarbide, D. Roye and M. Rodriguez, '*Unified Reference Frame Dq Model of the Brushless Doubly Fed Machine*', Proceedings of the Inst. Elect. Eng.- Electric Power Applications, Vol. 153, N°5, pp. 726 - 734, Sep. 2006.

[13] J. Poza, E. Oyarbide and D. Roye, '*New Vector Control For Brushless Doubly-Fed Machines*', in Proceedings of the IEEE-02, 28th Annual Conference of the Industrial Electronics Society, IECON, Vol. 2, N°3, pp. 1138 – 1143, Nov. 2002.

[14] M.B. Mohamed, M. Jemli, M. Gossa and K. Jemli, '*Doubly Fed Induction Generator (DFIG) in Wind Turbine Modelling and Power Flow Control*', IEEE International Conference on Industrial Technology, IEEE ICIT-04, Vol. 2, pp. 580 – 584, 2004.

[15] A. Dendouga, R. Abdessemed, M.L. Bendaas and A. Chaiba, '*Decoupled Active and Reactive Power Control of a Doubly-Fed Induction Generator (DFIG)*', Proceedings of the 15th Mediterranean Conference on Control & Automation, July 27-29, Athens, Greece, 2007.

[16] Y. Liu, L. Yi, H. Pan and Z. Lan, '*The Simulation Study for Brushless Doubly-Fed Generator Wind Power System Based on Fuzzy Control*', IEEE Power and Energy Engineering Conference, APPEEC, Asia-Pacific, pp. 1 - 4, March 2010.

[17] S. Jin, F. Zhang and Y. Li, '$H\infty$ *Robust Control for VSCF Brushless Doubly-Fed Wind Power Generator System*', Proceeding of the IEEE International Conference on Automation and logistics, ICAL'09, pp. 471 - 475, 2009.

[18] F. Zhang, S. Jin and X. Wang, 'L_2 *Robust Control for Brushless Doubly-Fed Wind Power Generator*', Proceeding of the IEEE International Conference on Automation and logistics, ICAL'09, pp. 1335 – 1339, Aug. 2009.

[19] X. Wang, J. Yang, X. Zhang and J. Wu, '*Sliding Mode Control of Active and Reactive Power for Brushless Doubly-Fed Machine*', Proceedings CCCM 08, International Colloquium on Computing, Communication, Control and Management, Vol. 2, pp. 294 – 298, Aug. 2008.

[20] I. Sarasola, J. Poza, M.A Rodriguez and G. Abad, '*Direct Torque Control for Brushless Doubly Fed Induction Machines*', IEEE International Conference of Electric Machines & Drives, Vol. 2, pp. 1496 - 1501, 2007.

[21] J. Poza, '*Modélisation, Conception et Commande d'une Machine Asynchrone Sans Balais Doublement Alimentée pour la Génération à Vitesse Variable*', PhD Dissertation, Institute National Polytechnique de Grenoble, Oct. 2003.

[22] P.C. Poberts, '*A Study of Brushless Doubly-fed (induction) Machines*', PhD. Dissertation, University of Cambridge. U.K, sep 2006.